(Supplement) Hyperspectral mapping of anisotropy

Meguya Ryu,[1] Reo Honda,[1] Armandas Balčytis,[2]
Jitraporn Vongsvivut,[3] Mark J. Tobin,[3] Saulius Juodkazis,[2,4,5] and Junko Morikawa[1]

[1] *Tokyo Institute of Technology, Meguro-ku, Tokyo 152-8550, Japan*
[2] *Nanotechnology facility, Swinburne University of Technology, John st., Hawthorn, 3122 Vic, Australia*
[3] *Infrared Microspectroscopy Beamline, Australian Synchrotron, Clayton, Victoria 3168, Australia*
[4] *Melbourne Center for Nanofabrication, Australian National Fabrication Facility Clayton 3168, Melbourne, Australia*
[5] *Tokyo Tech World Research Hub Initiative (WRHI), School of Materials and Chemical Technology, Tokyo Institute of Technology, 2-12-1 Ookayama, Meguro-ku, Tokyo 152-8550, Japan*

(Dated: May 22, 2019)

Equations in the Supplement are referenced to the main paper.

I. SUPPLEMENT

A. Test of the method with circular grating

First, the four-angle polarisation method was tested on a circular transmission grating inscribed through a 100 nm-thick Au film sputtered on a 30μm-thick sapphire (Tecdia, Ltd., Japan) using focussed ion beam (FIB, Raith IonLiNE). The grating had a deep-sub-wavelength $\Lambda = 0.2$ μm period (duty cycle 0.5) at the IR spectral range of 2.5 - 25 μm used in experiments (Fig. I.1). Absorbance was mapped at 18 θ angles (4 is enough for the method[1]) to improve fitting for the determination the orientation angle and amplitude, Amp (Eqn. 5). In this test, transmission through grooves of a constantly changing local orientation of the circular grating was measured. A single polariser configuration (Eqn. 2) was used.

Figure I.2 shows the transmittance, T, map (presented as absorbance $A = -\lg(T)$) at few IR wavelengths covering entire spectral range used in experiments. Transmittance is highest (A is lowest) at the location of the milled 50-μm-diameter grating (see, the inset for the actual sample made for this polarisation study). Increasingly stronger orientation amplitude was observed at the locations outwards from the center as expected from the geometrical curvature of the circular grating.

Some anisotropy in T (or A) is recognisable at shorter wavelengths (Fig. I.2) and is related to the sapphire substrate (c-cut) which has a none negligible absorbance even when using the thinnest crystalline sapphire substrate obtainable by mechanical polishing.

The transmission map shows clear image of anisotropy and its distribution dependent on the local curvature of the pattern over the single pixel of measurement.

B. Silk

A microtomed slice of silk $\sim$ 100 nm in thickness prepared on an IR-transparent non-birefringent substrate shows very well defined orientation of the absorption bands of silk (Fig. I.3). This slice is more that ten times thinner than was used previously for the molecular alignment measurement of the characteristic amide bands[2]: Amide II at 1512 cm^{-1} (C-N), Amide I β-sheets at 1628 cm^{-1} (C=O), and Amide A at 3290 cm^{-1} (N-H). Perpendicular orientation between C=O and C-N is revealed with high fidelity using longitudinal 100-nm-thick silk slices.

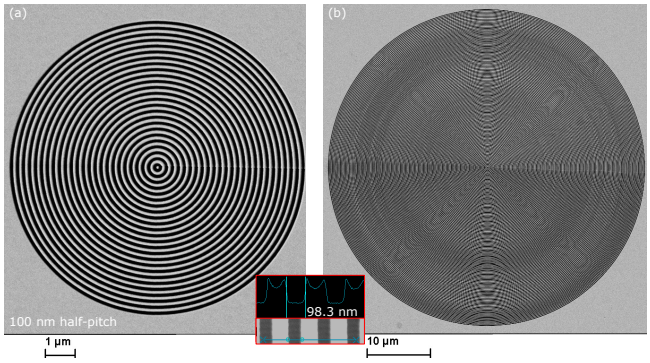

FIG. I.1: SEM images (top-view) of small 10 μm-diameter (a) and large 50 μm-diameter (b) circular grating with period $\Lambda =$ 200 nm and duty cycle 0.5 made by focussed ion beam (FIB) milling with Ga^+ ions in a 100 nm-thick Au film sputtered on a 30 μm thick sapphire.

C. Paracetamol

Paracetamol[3] was chosen for FT-IR hyperspectral mapping due to its well defined domain structure which has a phase retardance and absorption anisotropy. The Au circular grating and 100 nm-thick silk samples were tested for the absorbance and anisotropy measurements, however, they are show no retardance (silk with its strong birefringence is too thin). Hence, paracetamol was chosen to test possibility of simultaneous measurements of retardance and dihroism using equation Eqn. 4.

Paracetamol was melted between two 300 μm thick CaF_2 substrates and then quenched to the amorphous phase. Amorphous paracetamol was heated to 60°C and crystallized into form III[3]. Then, the form III was heated

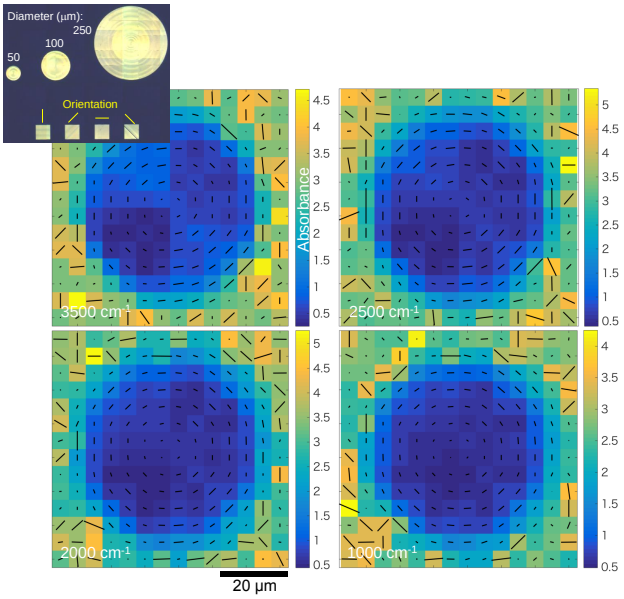

FIG. I.2: Absorbance superimposed with orientation maps of the 50 μm-diameter $\Lambda = 200$ nm and duty cycle 0.5 circular grating in Au on a c-cut 30 μm-thick sapphire (Fig. I.1 at few wavelengths; inset shows an optical image of the FIB-milled grating patterns used for the calibration). Measurement step 5 μm.

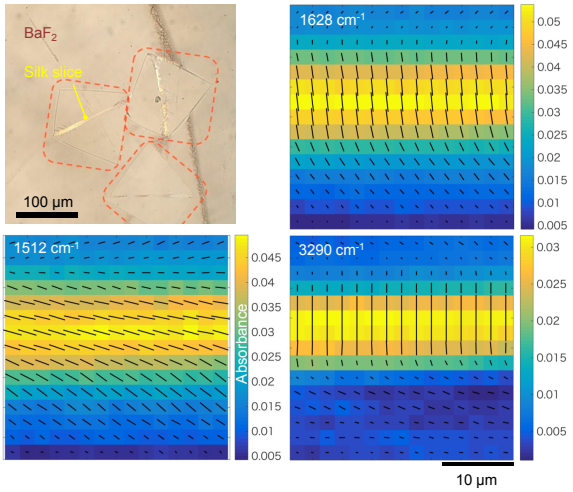

FIG. I.3: An optical image of longitudinal silk slices (see arrow) in epoxy made by microtome on BaF_2 substrate and absorbance maps at three representative bands overlayed with the orientation map. Thickness of the silk film $d = 0.1$ μm. At 1500 cm^{-1} (6.67 μm) wavelength $d/\lambda \simeq 1.5\%$. Scan step was 2 μm (pixel) measured at 4.1 μm resolution, which caused a poorly resolved silk-epoxy edge.

to 110°C and it was transformed into the Form II crystal which we used in this study.

Figure I.5 shows a summary of the absorbance mapping using the method based on Eqn. 2, which can only access the absorbance, hence $\kappa, \Delta\kappa$.

D. Poly-l-lactic acid (PLLA)

Poly-l-lactic acid (PLLA) forms a radial spherulite micro-crystals which have a simpler structural organisation when compared with poly-hydroxybutyrate (PHB) discussed in the main part of this study. The radial structure of PLLA micro-crystal formed between two CaF_2 plates is constrained and has the same orientational alignment along the entire cylindrical crystal of $10 - 14$ μm. The radial pattern is revealed by cross-polarised imaging shown together with representative spectrum of PLLA crystal in Fig. I.6.

Absorbance at selected wavelengths are shown with orientation maps overlaid on maps of the strength of absorption (the *Amp* amplitude) in Fig. I.7 and the birefringence with slow axis orientation in Fig. I.8.

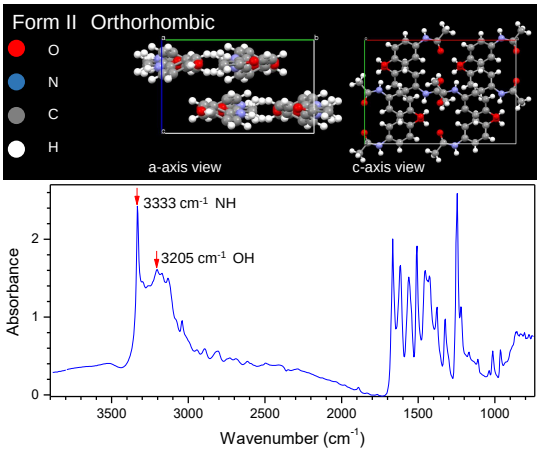

FIG. I.4: Paracetamol form II[3] crystal structure and absorbance spectrum averaged over the measured area at $\theta = 0°$. The hydrogen bonding band at 3205 cm^{-1} was used for the simultaneous Δn and $\Delta\kappa$ determination.

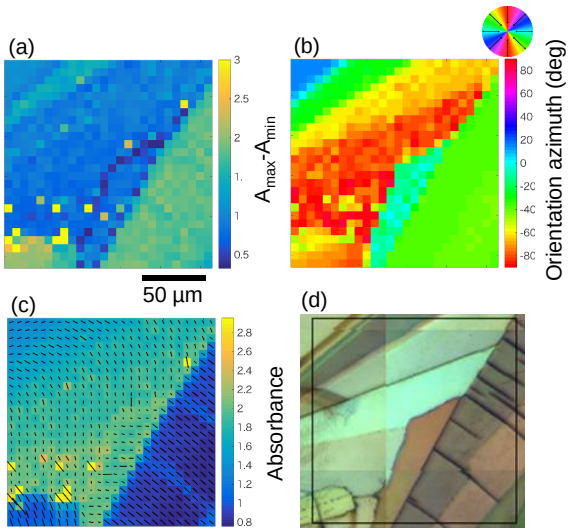

FIG. I.5: Paracetamol crystal imaged at the $\nu_{OH} = 3205$ cm^{-1} hydrogen bonding band using Eqn. 2. (a) The absorbance map at $\theta = 0$ deg. The color map amplitude $A_{max} - A_{min}$ was calculated from 8 angles (0, 15, 30, 45, 60, 75, 90, 135 deg). (b) The orientation θ_A map. (c) The averaged absorbance image from the $\theta = 0, 45, 90, 135$ deg maps with an overlayed vector plot. (c) Optical cross polarised imaged of the scanned area. Light source: synchrotron. Note: the new method based on Eqn. 4 is shown in the paper Fig. 6. Mapping pitch was 5 μm.

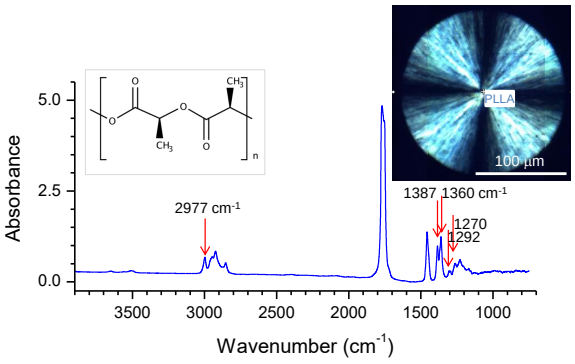

FIG. I.6: Absorbance spectrum of poly-l-lactic acid (PLLA) with marked bands at which mapping was carried out. Insets show cross polarised image of a spherulite and chemical formula of PLLA.

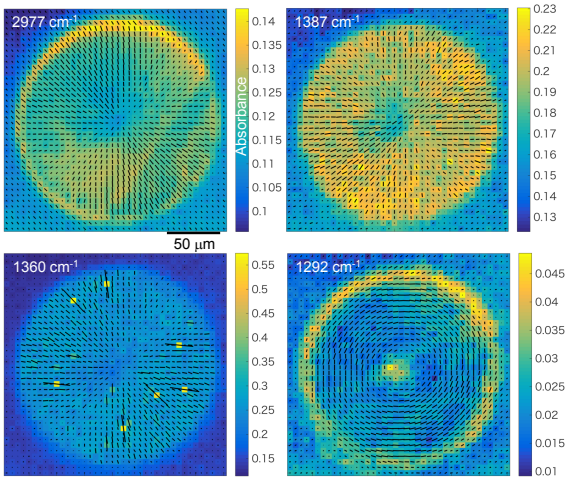

FIG. I.7: Absorbance and orientation maps of poly-l-lactic acid (PLLA) spherulite at few absorbance bands (marked in Fig. I.6). The absorption at 1270 cm^{-1} is an amorphous PLLA band.

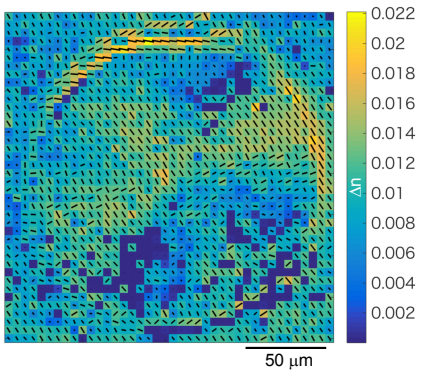

FIG. I.8: Birefringence, Δn, map and slow optical axis orientation at 2.6 μm wavelength. Thickness of cylindrical PLLA spherulite $d = 14.1$ μm. Slow axis is defined by the dipole moment direction.

[1] Y. Hikima, J. Morikawa, and T. Hashimoto, "FT-IR image processing algorithms for in-plane orientation function and azimuth angle of uniaxially drawn polyethylene composite film," *Macromolecules* **44**(10), pp. 3950 – 3957, 2011.

[2] M. Ryu, A. Bačytis, X. Wang, J. Vongsvivut, Y. Hikima, J. Li, M. J. Tobin, S. Juodkazis, and J. Morikawa, "Orientational mapping augmented sub-wavelength hyper-spectral imaging of silk," *Sci. Reports* **7**, p. 7419, 2017.

[3] M. Haisa, S. Kashino, and H.Maeda, "The orthorhombic form of p-hydroxyacetanilide," *Acta Cryst.* **B30**, pp. 2510 – 2512, 1974.